Neuron, Vol. 14, 717–730, April, 1995, Copyright © 1995 by Cell Press

Igf1 Gene Disruption Results in Reduced Brain Size, CNS Hypomyelination, and Loss of Hippocampal Granule and Striatal Parvalbumin-Containing Neurons

Klaus D. Beck,* Lyn Powell-Braxton,† Hans-R. Widmer,‡ Janet Valverde,* and Franz Hefti*‡
*Department of Neuroscience
†Department of Endocrine Research
Genentech, Incorporated
South San Francisco, California 94080
‡Andrus Gerontology Center
University of Southern California
Los Angeles, California 90089

Summary

Homozygous *Igf1*$^{-/-}$ mice at 2 months of age had reduced brain weights, with reductions evenly affecting all major brain areas. The gross morphology of the CNS was normal, but the size of white matter structures in brain and spinal cord was strongly reduced, owing to decreased numbers of axons and oligodendrocytes. Myelinated axons were more strongly reduced in number than unmyelinated axons. The volume of the dentate gyrus granule cell layer was reduced in excess of the decrease in brain weight. Among populations of calcium-binding protein-containing neurons, there was a selective reduction in the number of striatal parvalbumin-containing cells. Numbers of mesencephalic dopaminergic neurons, striatal and basal forebrain cholinergic neurons, and spinal cord motoneurons were unaffected. Cerebellar morphology was unaltered. Our findings suggest cell type- and region-specific functions for IGF-I and emphasize prominent roles in axon growth and maturation in CNS myelination.

Introduction

Insulin-like growth factor (IGF)-I, IGF-II, and insulin are members of the insulin gene family, and they stimulate cellular proliferation and differentiation during embryonic and postnatal development (Rechler and Nissley, 1990; Baker et al., 1993; Liu et al., 1993). The three proteins exhibit overlapping specificity for their receptors; IGF-I and insulin are the most potent ligands for, respectively, the IGF-I receptor and insulin receptor (Daughaday and Rotwein, 1989; Sara and Hall, 1990; Siddle 1992). The IGF-I receptor is a tyrosine kinase (Czech, 1989), and its interaction with IGF-I is modulated by a group of six known soluble high affinity IGF-I-binding proteins (IGFBP1–6; Ooi, 1990; Rechler and Brown, 1992; Clemmons et al., 1993). In the brain, IGFBP-2 is the most abundant binding protein and is present at high levels in the cerebrospinal fluid (Ocrant et al., 1990). In most brain areas, the temporal and spatial pattern of IGFBP-2 expression during embryonic and postnatal development closely resembles the expression of its IGF-I ligand, suggesting an important local interaction (Bondy et al., 1992; Lee et al., 1992, 1993). A similar correlation to the developmental expression of IGF-I has been reported for IGFBP-5 in other tissues, suggesting a role for the two binding proteins in targeting IGF-I to responsive cell populations (Bondy and Lee, 1993).

IGF-I promotes survival and stimulates neurite outgrowth from cultured central and peripheral neurons, including mesencephalic dopaminergic neurons, forebrain cholinergic neurons, and spinal cord motoneurons (Bothwell, 1982; Aizenman et al., 1986; Caroni and Grandes, 1990; Knüsel et al., 1990; Ang et al., 1992; Beck et al., 1993; Hughes et al., 1993; Neff et al., 1993). In vitro, IGF-I stimulates DNA synthesis and cell division of freshly dissociated neuroblasts, as shown for sympathetic cells (DiCicco and Black, 1988). Like a number of other factors, IGF-I increases the survival and myelin synthesis of cultured oligodendrocytes (Mozell and McMorris, 1991; Barres et al., 1992, 1993). A similar result has been obtained in vivo. Transgenic mice overexpressing IGF-I have larger brains, mostly owing to a strong up-regulation of oligodendrocyte myelin synthesis (Carson et al., 1993).

The correlation of the cell culture findings to the physiological role of IGF-I in vivo seems difficult to establish. Using Northern blotting analysis, *Igf1* mRNA levels in the rat brain have been found to be highest during late development and then to decline gradually to low adult levels (Rotwein et al., 1988). In situ hybridization and immunohistochemical studies indicate that *Igf1* mRNA is transiently expressed during development in many areas related to long projection neurons (Bondy, 1991; Garcia-Segura et al., 1991). The transient expression of IGF-I by projection neurons during axon growth and synaptogenesis has been taken to suggest an important role of IGF-I in these processes (Bondy, 1991). This speculation is supported by the permanent expression of IGF-I and its receptor in the olfactory bulb, where neuro- and synaptogenesis persists during adult life (Bondy, 1991).

Mice carrying inactive genes for IGF-I allow additional insights into the developmental functions of this trophic factor (Baker et al., 1993; Liu et al., 1993; Powell-Braxton et al., 1993). Homozygous *Igf1*$^{-/-}$ mice show strongly reduced perinatal survival and dwarfism due to generalized growth deficiency. In particular, at birth there is a strong reduction in the mass of skeletal muscle, bone, and organs and, in addition, delayed ossification and impaired development of lungs and epidermis (Baker et al., 1993; Powell-Braxton et al., 1993). The small percentage (<5%) of *Igf1*$^{-/-}$ mice that survive the perinatal period display unimpaired sucking behavior and feed normally after weaning. Recently, transgenic mice were generated that express human IGFBP-1 fused to the mouse metallothionein-I promoter (D'Ercole et al., 1994). Adult heterozygous mice display retarded brain growth manifested in a 8%–16% reduction of brain weight.

In this study, we report the results of a detailed anatomical analysis of the brains of *Igf1*$^{-/-}$ mice at 2 months of age.

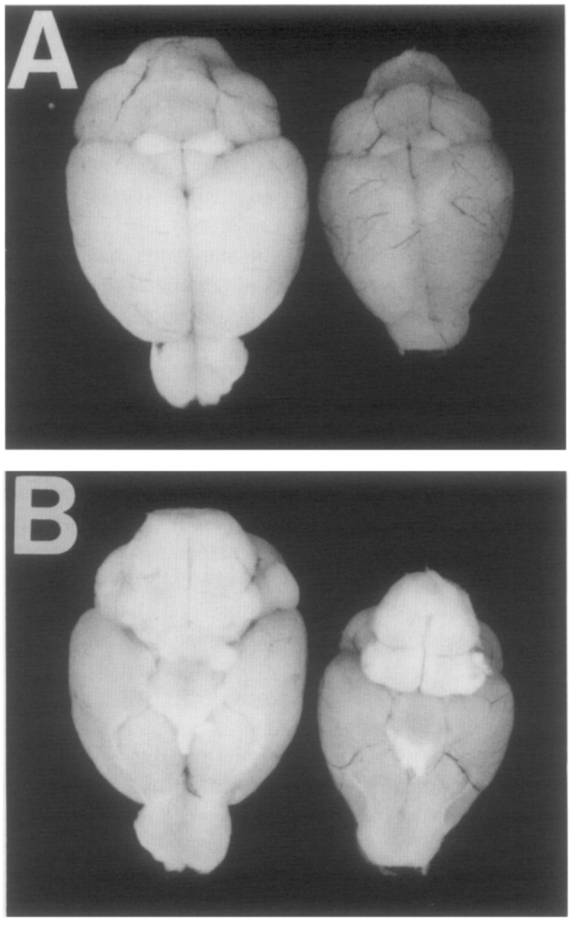

Figure 1. Comparison of Brains from *Igf1*$^{-/-}$ and Age-Matched Wild-Type Mice at P60

(A) Dorsal and (B) ventral views; IGF-1$^{-/-}$ brain is at right, and wild type is at left.

Results

Brain Weight and White Matter Axon Numbers and Axon Myelination Are Reduced in *Igf1*$^{-/-}$ Mice

The brains of *Igf1*$^{-/-}$ mice were smaller than those of age-matched wild-type mice (Figure 1). All major parts of the brain were present, and the sizes of all parts were reduced to similar extents as compared with wild type. The brain weights of *Igf1*$^{-/-}$ mice were 38% below weights of age-matched wild-type mice, whereas the body weights were reduced more dramatically, by 74% (Table 1). This differential effect of *Igf1* gene disruption resulted in a 2.3-fold increase in brain-to-body weight ratio.

The thickness of the anterior commissure, which contains axons connecting the left and right frontal lobes, was strongly reduced in *Igf1*$^{-/-}$ mice (Figure 2; Table 2). Histological staining for myelin with eriochrome cyanine R revealed a weakly stained fiber bundle that occupied a 69% smaller area than the same structure at a corresponding level in wild-type mice. This decrease was more than twice as much as the general reduction in brain size. Immunohistochemical staining with an antibody directed against oligodendrocyte membranes and CNS myelin (MAB328, Chemicon) showed a smaller and more weakly stained anterior commissure in *Igf1*$^{-/-}$ mice and thus confirmed the findings obtained with the histochemical method (Figures 2C and 2D). Adjacent sections stained with cresyl violet showed high packing density of nuclei in the brain parenchyma surrounding the anterior commissure in *Igf1*$^{-/-}$ mice, but in contrast, no increased density in the anterior commissure (Figures 2E and 2F).

Table 1. Body and Brain Weights

	Wild Type Weight (g)	*Igf1*$^{-/-}$ Weight (g)	Change(%)
Body	24.83 ± 1.25	6.55 ± 0.17	−74%[a]
Brain	0.46 ± 0.02	0.29 ± 0.01	−38%[a]
Ratio (brain to body)	1.9	4.4	+232%[a]

Body and brain weights of *Igf1*$^{-/-}$ and wild-type mice at 2 months of age. Brains were weighted after cutting off the medulla at the caudal end of pons. Values are means ± SEM of n = 5 (3 males, 2 females) for *Igf*$^{-/-}$ and n = 6 for wild-type brains (3 males, 3 females).
[a] Differs from wild type, $p < .001$.

The fiber bundles forming the internal capsule in the striatum and the corpus callosum showed the same dramatic reduction in thickness and myelin staining as the anterior commissure (Figures 2G–2J; Figures 3A–3D). The thickness of the medial part of the corpus callosum in *Igf1*$^{-/-}$ mice was reduced by 70% compared with corresponding anterior–posterior levels in wild-type mice (Table 2). In contrast, in the identical brain sections, the distance from the cortical to the basal surface of the brain and the thickness of the parietal cortex was only reduced by 30% and 26%, respectively.

Also in the spinal cord, the white matter areas were strongly reduced in size. Figures 3I (wild type) and 3J (*Igf1*$^{-/-}$) show transverse sections at the level of the fifth cervical root stained with eriochrome cyanine R and cresyl violet. The thickness of ventral, lateral, and dorsal funiculi was strongly reduced in *Igf1*$^{-/-}$ mice, whereas the size of the area occupied by gray matter was unaffected.

Immunohistochemical staining of oligodendrocytes was done using a rabbit antiserum directed against carbonic anhydrase II (CA II), which had been preabsorbed with brain extract of CA II-deficient mice. This antiserum selectively visualizes oligodendrocyte cell bodies (Ghandour et al., 1980; LeVine and Goldman, 1988). The staining revealed that the density of oligodendrocytes in white matter structures of *Igf1*$^{-/-}$ mice was unaffected (Figure 4 and Figure 5). Therefore, owing to the strong decrease in size of white matter, the total number of oligodendrocytes in *Igf1*$^{-/-}$ mice was strongly reduced.

Axon density and myelination in the anterior commissure and the medial part of the corpus callosum were analyzed using electron microscopy (Figure 6). In the medial corpus callosum, the density of myelinated axons decreased to 63.5% ± 5.1% (mean ± SEM of *Igf1*$^{-/-}$ mice compared with wild type), whereas the density of unmyelinated axons and the total axon density increased to 161.1% ± 10.2% and 132.8% ± 9.9%, respectively (Figure 7). In the anterior commissure, myelinated axon density decreased to 66.4% ± 7.1%, and the density of unmy-

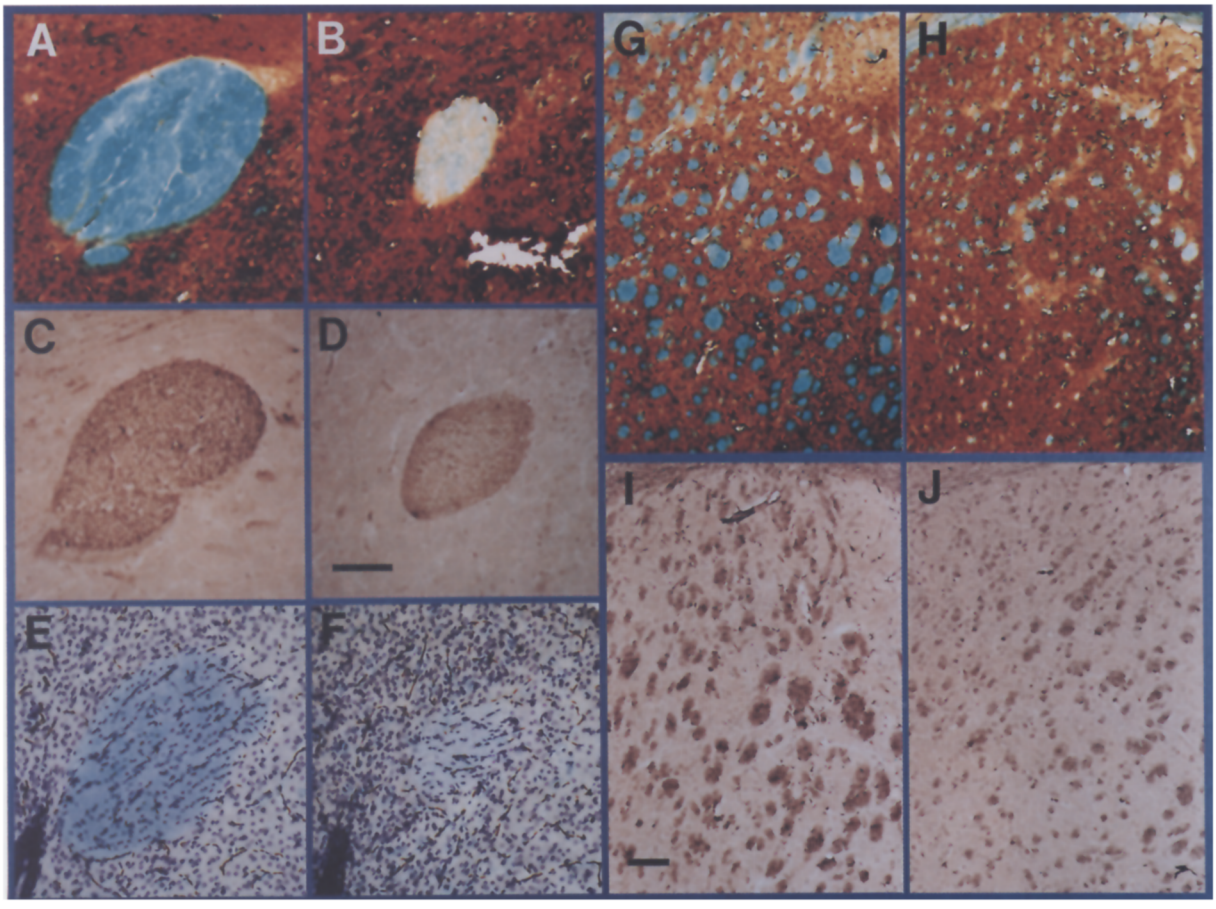

Figure 2. Anterior Commissure and Internal Capsule

Comparison of thickness and myelin content of anterior commissure and internal capsule fiber bundles in transverse brain sections at corresponding anterior-posterior levels from *Igf1*$^{-/-}$ (B, D, F, H, and J), and wild-type mice (A, C, E, G, and I).
(A–D and G–I) Histological myelin stain combined with immunohistochemical staining for calbindin D-28k (visualized with a HRP/diaminobenzidine method) to enhance the contrast (A, B, G, and H) and immunohistochemical staining of oligodendrocytes/myelin with MAB328 (C, D, I, and J). The thickness and myelin content of the anterior commissure is strongly reduced. (E and F) Cresyl violet staining.
Bars: 100 μm.

Table 2. Size of White Matter Tracts

	Wild Type	*Igf1*$^{-/-}$	Reduction (%)
Anterior commissure			
Area (mm^2)	0.91 ± 0.02	0.28 ± 0.02	69%[a,b]
Section area (mm^2)	40.39 ± 0.03	28.81 ± 0.03	29%[a]
Corpus callosum			
Thickness (mm)	0.35 ± 0.03	0.10 ± 0.01	70%[a,b]
Section cortical to basal			
Surface dist. (mm)	11.27 ± 1.03	7.51 ± 0.08	30%[a]
Parietal cortex			
Thickness (mm)	1.38 ± 0.10	1.02 ± 0.09	26%[a]

Areas and distances of 4 each wild-type and *Igf1*$^{-/-}$ mice were quantified in brain sections at corresponding anterior–posterior levels. For anterior commissure, corpus callosum, and comparative reference measurements, coronal sections from corresponding levels were used. Values are means ± SEM. The significance of differences was evaluated by Student's t test.
[a] Significantly different from wild type ($p < .05$).
[b] Different from reference measurement ($p < .01$).

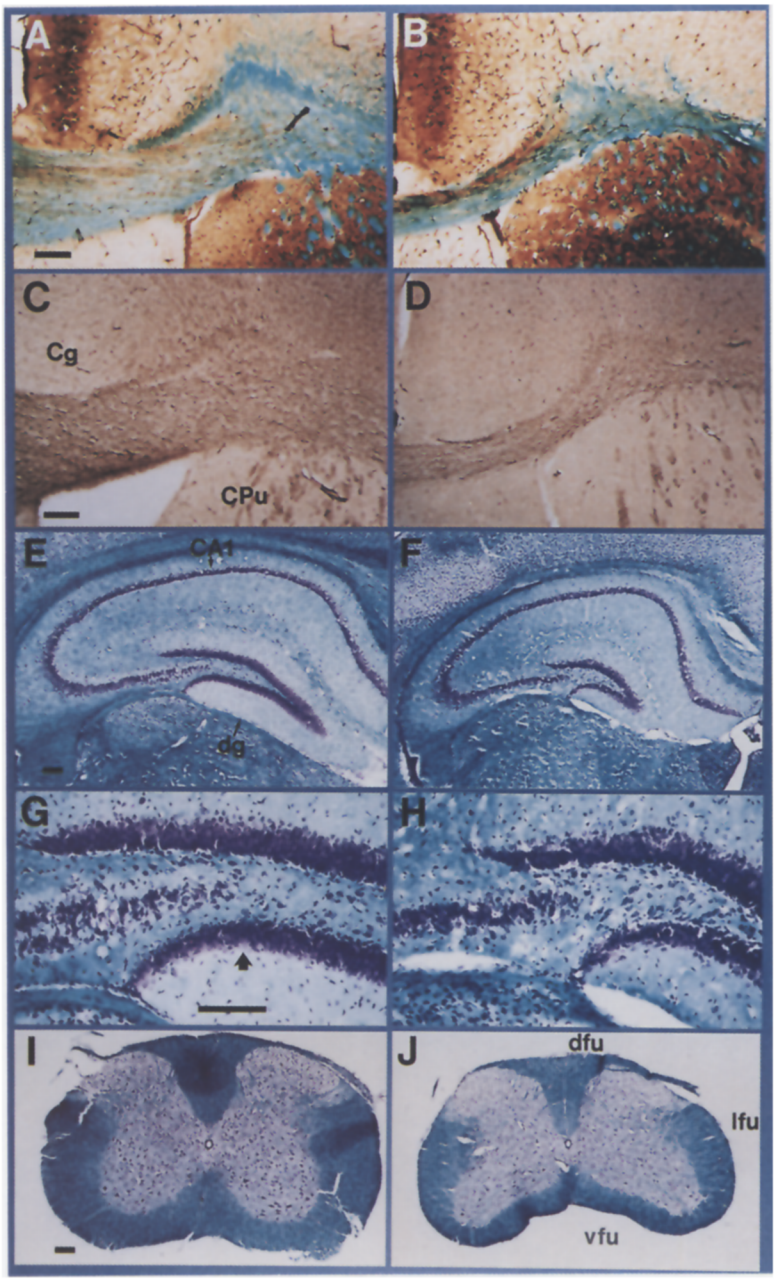

Figure 3. Corpus Callosum, Hippocampus, and Spinal Cord

Right column of photomicrographs (B, D, F, H, and J) is from *Igf1*$^{-/-}$ mice; left column (A, C, E, G, and I) is from wild-type mice. Eriochrome cyanine R staining combined with immunohistochemical staining for calbindin D-28k is shown in (A) and (B), and immunohistochemical staining with MAB328 is shown in (C) and (D). Thickness of corpus callosum is strongly reduced in *Igf1*$^{-/-}$ mice. Combined eriochrome cyanine R/cresyl violet staining of the dorsal hippocampus is shown in (E)–(H). Note strongly reduced size of the dentate gyrus (E and F), but identical thickness and packing density of dentate granule neuron cell body layers (arrow). (I) and (J) show combined eriochrome cyanine R/cresyl violet staining of spinal cord sections at level C4. Note the reduction in thickness of the white matter; dfu, lfu, and vfu designate the dorsal, lateral, and ventral funiculi, respectively, in *Igf1*$^{-/-}$ mice. CPu, caudate-putamen; Cg, cingulate cortex; dg, dentate gyrus; CA1, cornu ammonis area 1. Bars, 100 μm.

elinated and all axons increased to 139.6% ± 11.1% and 128.5% ± 8.1%, respectively.

The Volume of the Dentate Gyrus Cell Body Layer Is Reduced in *Igf1*$^{-/-}$ Mice

Visual inspection of the hippocampus suggested that the cell number in the dentate gyrus of *Igf1*$^{-/-}$ mice is strongly reduced, with more modest reductions in the CA1–4 areas (see Figures 3E and 3F). Cell bodies in the dentate gyrus were packed at very high density, as was made evident by a high density of nuclei in cresyl violet–stained sections. Both the packing density and the average size of nuclei in the dentate gyrus and CA1–4 was not significantly different in *Igf1*$^{-/-}$ and wild-type mice (see Figures 3G and 3H). Therefore, we estimated the changes in cell numbers in these areas by measuring and comparing the total volume occupied by their cell bodies (Table 3). The total volume of the area occupied by CA1–4 cell bodies, consisting mainly of pyramidal neurons, was reduced by 38%, which is identical to the decrease seen in overall brain weight (see Table 1). In contrast, the volume occupied by dentate gyrus cell bodies, which are almost exclusively dentate granule neurons, was reduced by 59% in *Igf1*$^{-/-}$ mice.

Parvalbumin-Containing Neurons Are Lost in a Region-Dependent Manner

Parvalbumin-containing neurons were counted in the striatum and the hippocampus (Table 4; Figure 8; see Figure

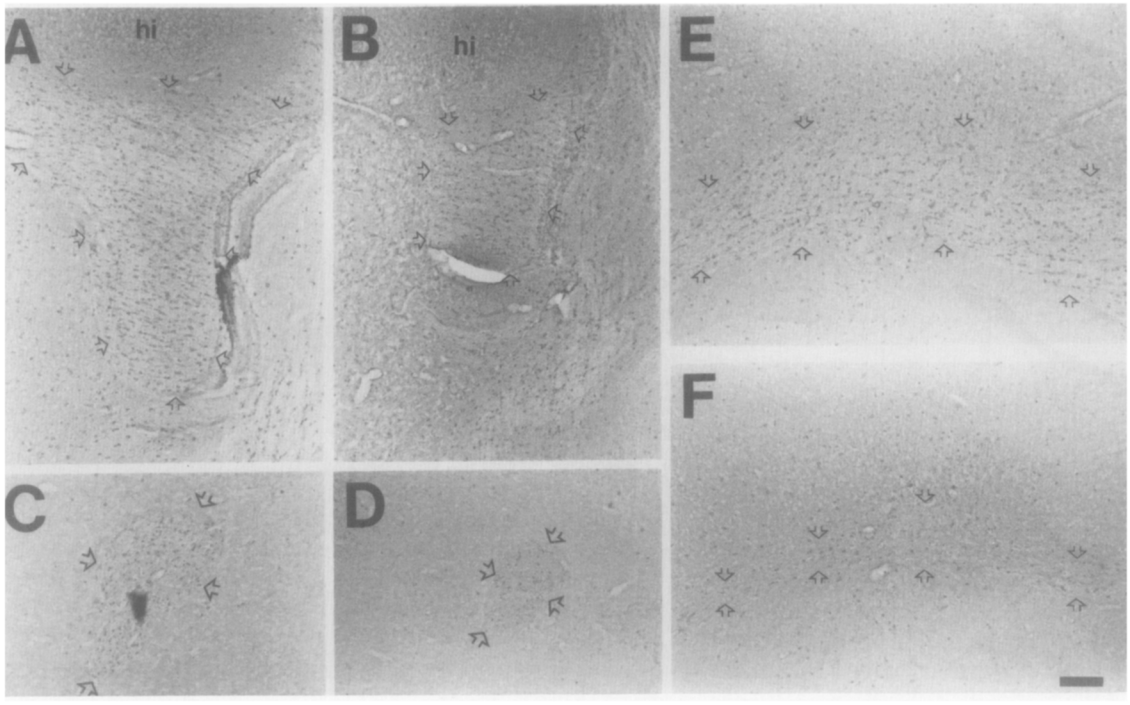

Figure 4. Oligodendrocytes in White Matter Structures

Brain sections from corresponding anterior–posterior levels of *Igf1*$^{-/-}$ (B, D, and F) and wild-type mice (A, C, and E) were immunoperoxidase stained with a CA II antiserum that had been preabsorbed with brain extract from a CA II–deficient mouse strain. Only cell bodies are stained. Fimbria (A and B), anterior commissure (C and D), and corpus callosum (E and F) are delineated by arrows. Note identical density of labeled oligodendrocytes within white matter in *Igf1*$^{-/-}$ and wild-type mice. hi, hippocampus. Bars, 100 μm.

10). In the hippocampus, the numbers were reduced in *Igf1*$^{-/-}$ mice by 32% and 35% in CA1–4 areas and the dentate gyrus, respectively. In contrast, in the dorsal striatum, the decrease was 52%, which was significantly stronger than in the hippocampus. This was not simply due to a stronger reduction of the overall striatal volume in *Igf1*$^{-/-}$ mice. The striatal volume estimated from serial sections was decreased by 28%, whereas the volumes occupied by the CA1–4 and dentate gyrus cell bodies were reduced by 38% and 59%, respectively (Table 3 and Table 4). Therefore, the number of parvalbumin immunopositive neurons in the striatum was more strongly decreased relative to the striatal volume than in the CA1–4 areas, whereas they were less reduced in the dentate gyrus.

The thickness of parietal cortex was reduced in *Igf1*$^{-/-}$ mice (see Table 2). Both overall cell density and the density of parvalbumin immunoreactive neurons in all cortical areas was increased, most evidently in layers IV and VI (Figure 9, parietal cortex shown). To assess the number of cortical projection neurons, which participate in the formation of white matter tracts, we established the density of neurons with large nuclei in Nissl-stained 40 μm thick sections of parietal and temporal cortex layers III and V. In layer III, neuron densities in wild-type and *Igf1*$^{-/-}$ mice were 1340 ± 180 and 2090 ± 320 cells/mm^2 (mean ± SD; n = 3), respectively, amounting to a 56% increase in *Igf1*$^{-/-}$ mice. In layer V, the corresponding values were 1180 ± 110 and 1860 ± 210 cells/mm^2, resulting in a 57% increase in density in *Igf1*$^{-/-}$ mice as compared with wild-type animals. This increase in cell density is comparable with the decrease in cortical volume (see Table 2), suggesting that the total number of cortical projection neurons remained unchanged.

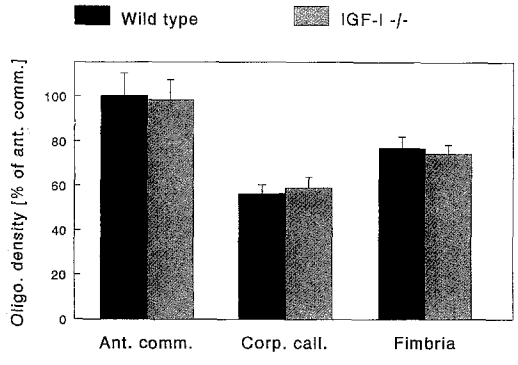

Figure 5. Density of Oligodendrocytes in Forebrain White Matter Structures

Brain sections were immunostained for CA II, and oligodendrocyte cell bodies were counted in anterior commissure, corpus callosum, and fimbria of *Igf1*$^{-/-}$ and wild-type mice. Areas used for counting were measured with an image analysis system. Data are means ± SEM from four *Igf1*$^{-/-}$ and four wild-type mice, expressed as percentage of the density measured in the anterior commissure.

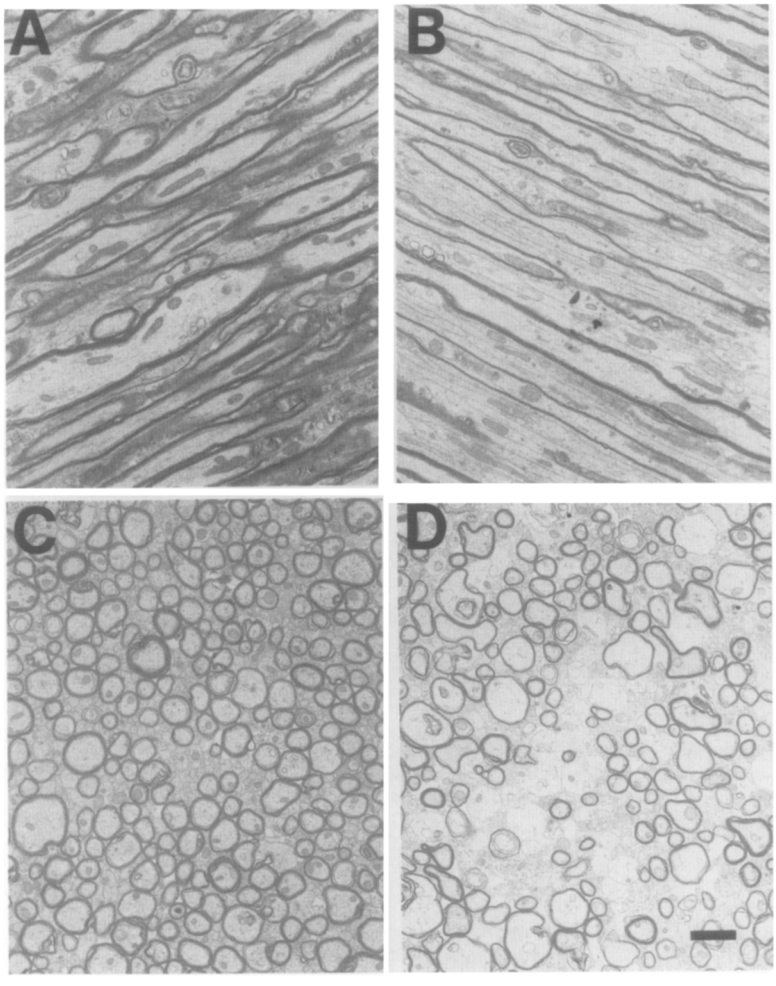

Figure 6. Myelination of CNS White Matter Tracts

Electron micrographs of longitudinal (A and B) and cross-sections through the medial corpus callosum of wild type (A and C) and *Igf1*$^{-/-}$ (B and D). Note reduced density of myelinated axons in *Igf1*$^{-/-}$ sections. Bar, 1 μm.

The Distribution of Astrocytes Immunopositive for Glial Fibrillary Acidic Protein and of Neurons Containing Calbindin D-28k and Calretinin Is Unaffected in *Igf1*$^{-/-}$ Mice

The distribution and staining intensity of glial fibrillary acidic protein (GFAP) immunopositive astrocytes was identical in all brain areas of wild-type and *Igf1*$^{-/-}$ mice (Figure 10, only hippocampus shown). Because of the regional changes seen in the numbers of parvalbumin-containing neurons, we analyzed the expression of calbindin D-28k and calretinin, two other cytoplasmatic calcium-binding proteins. In contrast to the situation found for parvalbumin, the distribution and the staining intensity of identified neurons was unaltered in all areas examined (Figures 10E–10H, only hippocampus shown). Therefore, the decrease in the number of calbindin D-28k and calretinin immunopositive neurons was proportional to the decrease in volume of the respective brain area.

The Numbers of Cholinergic and Dopaminergic Neurons and Spinal Cord Motoneurons Are Unaffected

The decrease in cell numbers in IGF$^{-/-}$ mice did not include all neuronal populations. Numbers of striatal and basal forebrain choline acetyltransferase (ChAT) immunopositive cholinergic neurons, ventral mesencephalic tyrosine hydroxylase (TH) immunopositive dopaminergic neurons, and the numbers of motoneurons in lumbar spinal segments L4 and L5 were not significantly different in *Igf1*$^{-/-}$ and wild-type mice (Table 4).

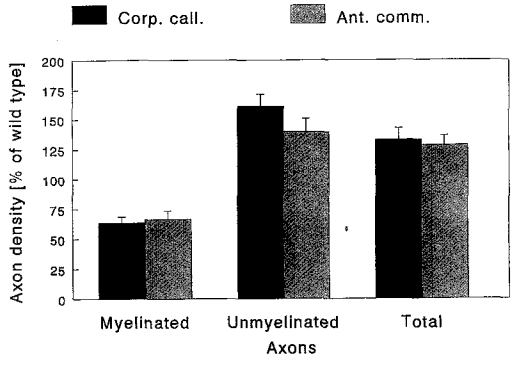

Figure 7. Axon Densities in White Matter Tracts

Numbers of myelinated, unmyelinated, and total axons were counted within standardized areas of anterior commissure and medial corpus callosum as described in Experimental Procedures. Data are means ± SEM expressed as percentage of the means in wild-type littermates. All values are significantly different from wild type ($p < .05$, Student's t test; $n = 3$).

Table 3. Volume of Hippocampal CA1–4 Pyramidal and Dentate Granule Neuron Cell Body

	Wild Type	*Igf1*$^{-/-}$	Reduction (%)
CA1–4 (mm^3)	17.7 ± 1.1	10.9 ± 0.7	38%[a]
Dentate (mm^3)	7.3 ± 0.4	3.0 ± 0.4	59%[a,b]
Ratio (dentate to CA1–4)	0.42	0.28	33%[a]

Serial transverse sections (40 μm) through the entire extent of the hippocampus in 4 each wild type and *Igf1*$^{-/-}$ mice were stained with cresyl violet, and volumes occupied by cell bodies of CA1–4 pyramidal and dentate granule neurons were determined as described in Experimental Procedures. Statistical significance was evaluated by Student's t test.

[a] Significantly different from wild type ($p < .05$).

[b] Different from reduction of CA1–4 volume ($p < .01$).

Discussion

The majority of homozygous *Igf1*$^{-/-}$ mice die perinatally, and the survivors have an approximately 75% reduction in body weight when analyzed at 2 months of age. The present study established a less severe reduction in brain weight (38%) distributed evenly over all major brain areas. However, detailed histological analysis revealed region and cell type–dependent effects of the *Igf1* gene disruption. Most evident was the strong reduction in size of the two major white matter structures of the forebrain, the anterior commissure and corpus callosum, which were reduced by approximately 70% compared with wild-type littermates. Also, the fiber bundles of the internal capsule, fimbria, and spinal cord white matter were strongly affected. However, the densities of oligodendrocytes determined in anterior commissure, corpus callosum, and the fimbria were unaltered in *Igf1*$^{-/-}$ mice. Therefore, the total number of oligodendrocytes in these white matter structures was reduced proportionally to their decrease in size. The density of myelinated axons within the anterior commissure and corpus callosum was decreased by about 35% in *Igf1*$^{-/-}$ mice, whereas the densities of unmyelinated and total axons were increased by 40%–61% and 28%–33%, respectively (see Figure 7). These findings amount to a net loss of axons, with a strong shift in prevalence from myelinated to unmyelinated fibers. Therefore, *Igf1* gene inactivation affects both the number of axons forming white matter tracts and their myelination by oligodendrocytes. Cell bodies of projection neurons in cerebral cortex layers III and V, which send axons through corpus callosum, were not lost proportionally to the decrease in axon numbers. This finding suggests a role for IGF-I in axonal growth and/or maturation. Such a role has been proposed based on the developmental expression patterns of IGF-I, the IGF-I receptor, and binding proteins in large projection neurons and surrounding glial cells (Bondy, 1991; Bondy et al., 1992; Lee et al., 1992; Bondy and Lee, 1993). In addition, several studies have shown that IGF-I promotes neurite growth in embryonic neurons in vitro (Aizenman and De Vellis, 1987; Caroni and Grandes, 1990; Beck et al., 1993). Further support for a role for IGF-I in axon growth is based on its function as a mediator of growth hormone actions during postnatal development (Froesch et al., 1985; Mathews et al., 1986; Fagin et al., 1989; Daughaday, 1989) and the findings that numbers and lengths of CNS axons and dendrites are reduced in the growth hormone–deficient Snell dwarf and little mice (see review, Noguchi, 1991). Both mouse mutants also show CNS hypomyelination associated with strongly decreased

Table 4. Neuronal Counts

	Wild Type	*Igf1*$^{-/-}$	Reduction (%)
Parvalbumin positive cells			
Striatum	9,204.3 ± 566.2	4,446.0 ± 302.8	52%[a,b]
Hippocampus			
CA1–4	4,402.6 ± 283.6	3,108.3 ± 304.1	32%[a]
Dentate gyrus	486.0 ± 42.4	200.9 ± 19.9	59%[a,b]
Striatal volume (mm^3)	112.9 ± 8.2	81.3 ± 7.8	28%[a]
ChAT positive cells			
Striatum	23,160.4 ± 1,785.3	22,534.0 ± 2,025.2	Not significant
Basal forebrain	3,332.4 ± 310.6	3,134.0 ± 219.2	Not significant
TH positive cells			
Ventral mesencephalon	16,302.1 ± 1,801.7	15,251.3 ± 1,609.9	Not significant
Spinal cord motoneurons (L4–5)	1,103.3 ± 119.4	996.7 ± 89.0	Not significant

Immunopositive neurons were counted in every sixth of serial sections (40 μm) from 4 each of wild-type and *Igf1*$^{-/-}$ mice, covering the entire anterior–posterior extent of striatum (paravalbumin, ChAT), hippocampus (parvalbumin), basal forebrain (ChAT), and ventral mesencephalon (TH). Striatal volume was estimated based on striatal area measurements in serial coronal sections through the entire anterio–posterior extent of caudate putamen and globus pallidum, as described in Experimental Procedures. Spinal cord motoneurons were counted in every fifth of serial transverse sections (18 μm) from 3 *Igf1*$^{-/-}$ and 3 wild-type mice. Values are means ± SEM.

[a] Different from wild type, $p < 0.001$.

[b] Different from reductions in CA1–4 ($p < 0.01$; Student's t test).

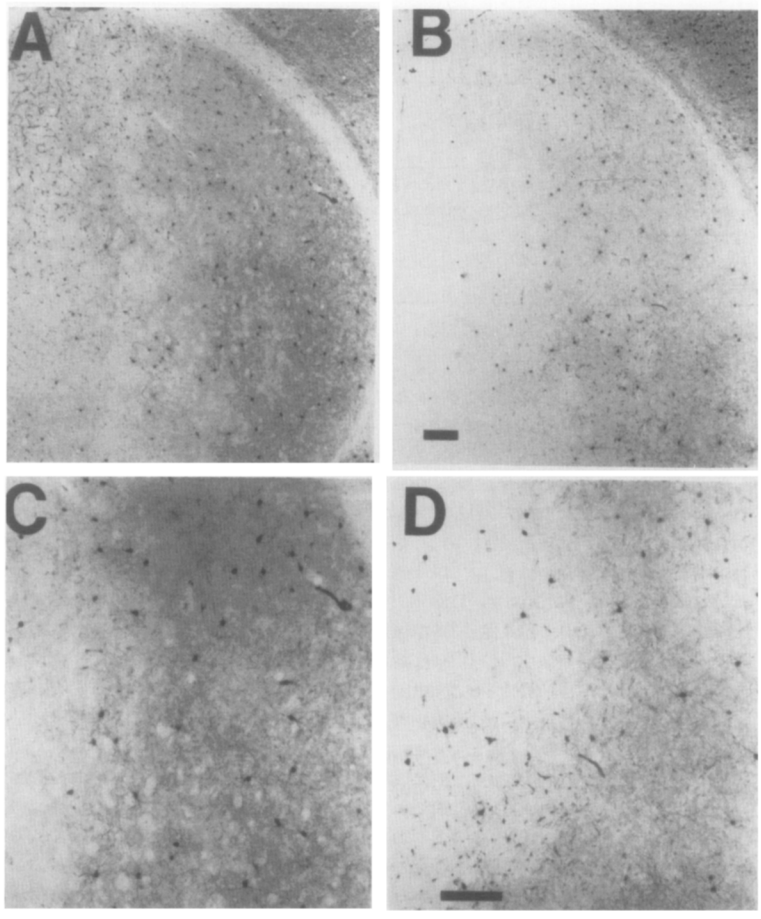

Figure 8. Parvalbumin-Expressing Striatal Neurons

Dorsal striatum of *Igf1*$^{-/-}$ (B and D) and age-matched wild-type mice (A and C) stained with parvalbumin antibodies. (C) and (D) show magnified areas from (A) and (B). Note the reduced density of stained neurons in (A) and (C). Bars, 100 μm.

numbers of oligodendrocytes, suggesting an important role for IGF-I in myelination (Noguchi et al., 1982a, 1982b, 1985; Sugisaki et al., 1985; King et al., 1988).

In mice CNS, myelination occurs during the first 4 postnatal weeks, with an initial period of oligodendrocyte proliferation and a partially overlapping consecutive period of myelin synthesis (Morell et al., 1972; Matthieu et al., 1973). There is evidence that the number of oligodendrocytes is developmentally regulated by axons (Barres and Raff, 1994). Studies on optic nerve myelination have shown that the proliferation of oligodendrocyte precursors is dependent on the presence of electrically active axons that might produce or release an unidentified growth factor (Gyllensten and Malmfors, 1963; Tauber et al., 1980; Barres and Raff, 1993). In addition, the axon number also regulates the survival of oligodendrocytes during normally occurring developmental cell death (Barres et al., 1993). These findings suggest that the decrease in the numbers of oligodendrocytes we found in white matter tracts of *Igf1*$^{-/-}$ mice is secondary to the reduced number of axons. However, there is also strong evidence for a direct effect of the *Igf1* gene inactivation on oligodendrocytes. The density of oligodendrocytes in the anterior commissure and corpus callosum is unaltered, but the density of myelinated axons is decreased by approximately 35%, with a concomitant increase in the density of unmyelinated fibers. Therefore, in addition to a function of IGF-I for brain growth and maturation, our findings demonstrate the importance of IGF-I for myelination in vivo and are in line with many studies demonstrating that IGF-I stimulates oligodendrocyte survival, development, and proliferation in vitro (McMorris et al., 1986, 1990; McMorris and Dubois-Dalcq, 1988; Mozell and McMorris, 1991; Barres et al., 1992). Oligodendrocytes and their precursors express IGF-I receptors (McMorris et al., 1986, 1990). Recently, Carson et al. (1993) reported a 130% increase of brain myelin content at postnatal day 55 (P55) in a transgenic mouse line overexpressing IGF-I under a mouse metallothionein promoter. The number of oligodendrocytes was unaltered in these mice, suggesting that overexpressed IGF-I stimulated the synthesis of myelin.

Our findings provide direct evidence for a decrease in the number of oligodendrocytes in *Igf1*$^{-/-}$ mice, but the fact that myelination was not completely abolished in our *Igf1*$^{-/-}$ mice clearly demonstrates that IGF-I is not absolutely required for this process. The lack of IGF-I might be partially compensated by IGF-II, which is abundantly expressed in choroid plexus, meninges, and vascular cells from early development to maturity and is released into the cerebrospinal fluid (Stylianopoulou et al., 1988; Hynes et al., 1988; Bondy et al., 1992). In addition, IGF-II, which during prenatal development is secreted by the liver into the bloodstream, and insulin can enter the brain (Hodgkinson et al., 1991). The issue of whether IGF-II compensates

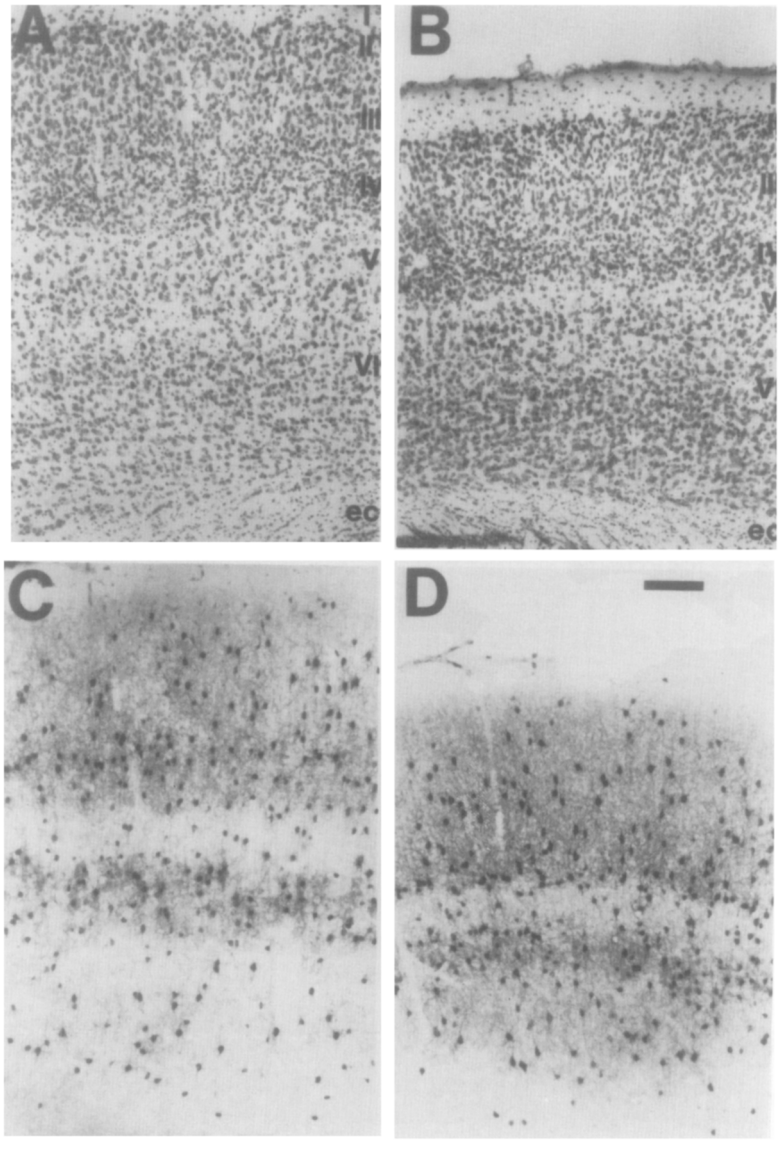

Figure 9. Cerebral Cortex with Parvalbumin-Expressing Neurons

Parietal cortex of *Igf1*$^{-/-}$ (B, D) and wild-type (A, C) mice. Cresyl violet staining (A and B) and parvalbumin immunohistochemistry (C and D) on adjacent sections. In (A) and (B), the cortical layers are labeled. Note the reduced overall thickness, the more tight packing of cell bodies in *Igf1*$^{-/-}$ cortex, in particular in layers IV and VI (B), and the higher density of parvalbumin-containing neurons in layer IV. ec, external capsule. Bar, 100 μm.

for IGF-I in *Igf1*$^{-/-}$ mice can be addressed in *Igf1*$^{-/-}$/*Igf2*$^{-/-}$ double mutants (Baker et al., 1993; Liu et al., 1993), but a neuropathological characterization of such mutant mice has not been reported.

In vitro lineage studies suggest that oligodendrocytes and type 2 astrocytes are both derived from a common O-2A progenitor cell (see reviews, Collarini et al., 1991; Noble et al., 1991; Noble and Wolswijk, 1992). Treatment of O-2A progenitor cells with IGF-I promotes the proliferation of oligodendrocytes and oligodendrocyte precursors, but does not increase the numbers of type 2 GFAP immunopositive astrocytes. In vitro, ciliary neurotrophic factor induces differentation of O-2A progenitors into type 2 astrocytes (Hughes et al., 1988). Although the significance of these cell culture studies for the in vivo situation is unclear, our finding that the distribution and relative abundance of GFAP immunopositive astrocytes in *Igf1*$^{-/-}$ mice is not different from wild type clearly demonstrates that the differentiation of astrocytes in vivo can occur in the absence of IGF-I.

Decreases proportional to the 38% loss of brain weight in *Igf1*$^{-/-}$ mice were found for the numbers of calbindin- and calretinin-containing neurons and for the total volume occupied by the striatum and hippocampal CA1–4 cell bodies. Numbers of cortical and hippocampal parvalbumin immunopositive neurons were also reduced by approximately 30%, but in the dorsal striatum, they were decreased by 52%. In contrast, the numbers of TH immunopositive neurons in the ventral mesencephalon, striatal and basal forebrain cholinergic neurons, and spinal cord motoneurons were unaffected by disruption of the *Igf1* gene.

The overall decrease in total brain weight and the volumes occupied by the striatum and hippocampal CA1–4 cell bodies in *Igf1*$^{-/-}$ mice was exceeded by the 59% reduction in the volume of the dentate gyrus granule cell body layer.

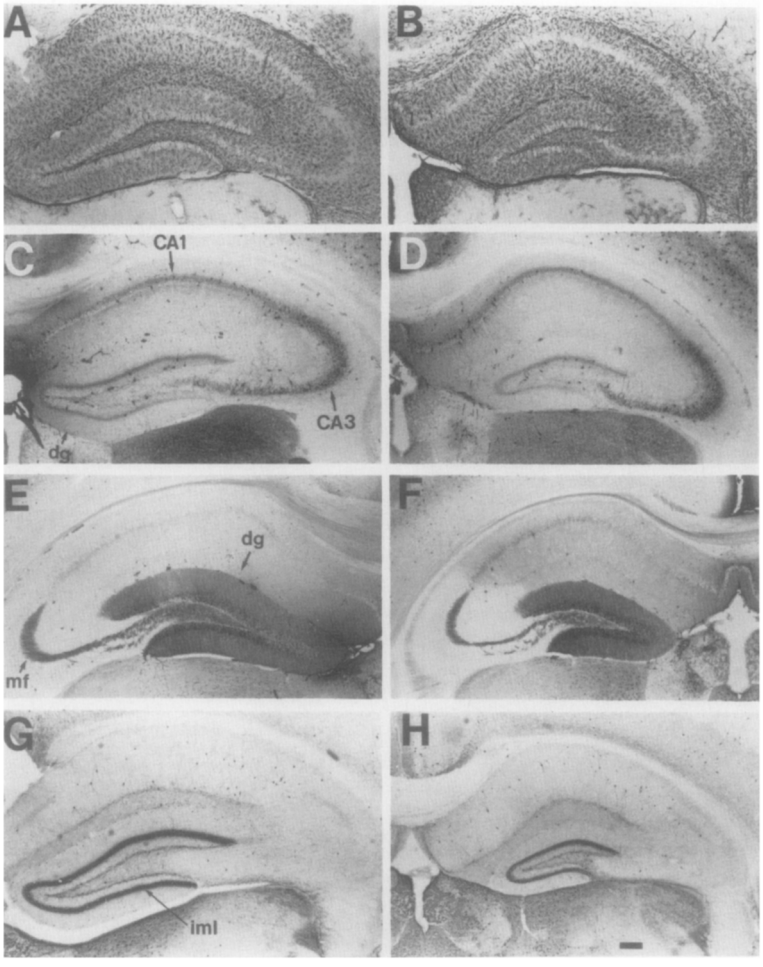

Figure 10. GFAP, Parvalbumin, Calbindin D-28k, and Calretinin Expression in the Hippocampus

Left column of photomicrographs, wild type; right column, *Igf1*$^{-/-}$ mice.

Immunohistochemistry for GFAP (A and B), parvalbumin (C and D), calbindin D-28k (E and F), and calretinin (G and H) shows identical distribution, neuron numbers, and staining intensity in wild-type and *Igf1*$^{-/-}$ mice. Note the reduced size of the dentate gyrus (dg) in *Igf1*$^{-/-}$. CA1/3, cornu ammonis regions 1/3; mf, mossy fibers. Bar, 100 μm.

This finding suggests an involvement of IGF-I in the generation of dentate granule neurons. The majority of these cells are generated during early postnatal life, whereas hippocampal pyramidal neurons, the principal cells in CA1–4, are born between embryonic day 16 (E16) and E20 (Altman and Bayer, 1990a, 1990b). The expression of *Igf1* mRNA in the rat brain peaks around late embryonic to early postnatal developmental time points (Bondy, 1991; Lee et al., 1993). Within the developing hippocampus, IGF-I receptor mRNA is expressed in all neurons, whereas *Igf1* mRNA is present in a small subset of evenly distributed interneurons. IGFBP-5 is expressed postnatally in dentate granule neurons (Bondy and Lee, 1993), suggesting that IGF-I, in interaction with IGFBP-5, plays an important role in the generation of dentate granule neurons. The morphology of dentate granule neurons as visualized by Nissl staining in *Igf1*$^{-/-}$ mice was not different from wild type. Calbindin immunostaining pattern and intensity was unaffected, and calretinin-containing terminals originating from the hypothalamic supramammillary nucleus (Résibois and Rogers, 1992) terminated in the same dendritic area. However, the numbers of parvalbumin immunopositive neurons in the dentate gyrus were relatively spared from the overproportional decrease in volume.

A detailed analysis of developmental growth in mice with single or combined null mutations of the IGF-I, IGF-II, and IGF-I receptor genes has suggested that before E13.5, the IGF-I receptor exclusively mediates the biological effects of IGF-II, and later with increasing IGF-I expression, interacts with both IGFs (Baker et al., 1993). Therefore, IGF-I seems to play a more important role during late embryonic and postnatal development. To analyze whether disruption of the *Igf1* gene generally affected CNS structures that are generated relatively late during development (dentate gyrus, white matter), we studied the morphology of the cerebellum. In rats, Purkinje cells, the cerebellar projection neurons, are born and have migrated to their final locations by E17. At the time of birth, a transient germinal zone forming the external granular layer is the birthplace of granule neurons. These cells proliferate and migrate until approximately P20. Concomitantly, Purkinje neurons mature and form extensive dendritic arbors, which receive numerous synaptic contacts from granule neurons and the inferior olive. IGF-I receptor mRNA is widely expressed in the cerebellar cortex (Bondy et al., 1992). From P4 to P21, Purkinje neurons express high levels of *Igf1* mRNA (Bondy, 1991), whereas adjacent Bergmann glial cells contain IGFBP-2 mRNA (Lee et al., 1992), and proliferating cells in the external granular layer

express IGFBP-5 mRNA (Bondy and Lee, 1993). IGF-I is a potent mitogen for cerebellar granule cell neuroblasts in vitro (Gao et al., 1991). In contrast to these findings, which strongly suggest an involvement of IGF-I in cerebellar development, the morphology, anatomical organization, and relative abundance of Purkinje and granule neurons in *Igf1*$^{-/-}$ mice was unaffected (data not shown). The cerebellum was decreased in size proportional to the overall reduction in brain weight and size.

Our findings of cell type– and region-specific changes in *Igf1*$^{-/-}$ mice suggest that IGF-I plays a role in the differentiation of some CNS cells, whereas others are not dependent on its presence. The numbers of parvalbumin-containing neurons in the cortex and the CA1–4 regions of the hippocampus were reduced proportionally to the general decrease in weight and cell number. In the dentate gyrus, the reduction was less than proportional. In contrast, the loss of parvalbumin immunopositive neurons in the dorsal striatum was almost twice as much as that seen in the other brain areas. The distribution of neurons expressing calbindin and calretinin, two other calcium-binding proteins, was unaffected in *Igf1*$^{-/-}$ mice in all brain areas studied, and their numbers were decreased proportional to the reduction of brain weight and volume.

The exact functions of the calcium-binding proteins calretinin, calbindin, and parvalbumin are still largely unknown. It has been suggested that they act as intracellular Ca^{2+} buffers and that they are directly involved in Ca^{2+} signal transduction processes (Mattson et al., 1991; Baimbridge et al., 1992). In the cerebral cortex and the hippocampus, parvalbumin is expressed by a subset of GABAergic neurons that display, at least in the hippocampus, a rapid firing rate and high metabolic activity (Celio 1984, 1990; Bergmann et al., 1991; Solbach and Celio, 1991). The exact transmitter type of striatal parvalbumin immunoreactive neurons is not known, but they are most likely not GABAergic (Celio, 1990). Therefore, the regional difference in the loss of parvalbumin-containing neurons in *Igf1*$^{-/-}$ mice reflects a difference in the dependency of distinct cell types on the trophic factor.

Numbers of basal forebrain cholinergic neurons, mesencephalic dopaminergic neurons, and large spinal cord motoneurons in *Igf1*$^{-/-}$ mice were not significantly different from those in wild-type mice. These findings are rather surprising considering the large amount of data suggesting an important role for IGF-I in the development of these sets of neurons. In cell culture systems, IGF-I promotes survival of mesencephalic dopaminergic and forebrain cholinergic neurons and stimulates neurite outgrowth and survival of spinal cord motoneurons (Knüsel et al., 1990; Ang et al., 1992; Beck et al., 1993; Hughes et al., 1993). IGF-I is present in developing muscle fibers (Ralphs et al., 1990) and has been shown to induce motoneuron axonal sprouting and regeneration and to protect against nerve transection–induced degeneration (Caroni and Grandes, 1990; Neff et al., 1993). When administered during the period of naturally occurring, developmentally regulated neuronal death, IGF-I rescued a significant number of chick motoneurons (Neff et al., 1993). The absence of a significant change in spinal cord motoneuron number is even more surprising, considering the profound reduction in muscle mass in *Igf1*$^{-/-}$ mice (Powell-Braxton et al., 1993), which suggests that the production of other muscle-derived trophic factors like brain-derived neurotrophic factor, neurotrophin-3, and neurotrophin-4/5 (Henderson et al., 1993) might be decreased. However, muscle fibers are most likely not the only source of trophic support for developing motoneurons. This function might be shared by other CNS/PNS neurons and glial cells that are in close contact to motoneurons in vivo, exerting social control of survival (Eagleson et al., 1985; Eagleson and Bennett, 1986; Raff, 1992; Hughes et al., 1993). Similar compensatory effects by other trophic factors and mechanisms might explain the absence of a change in the numbers of mesencephalic dopaminergic and basal forebrain cholinergic neurons.

Taken together, at the present level of analysis, our findings indicate a prominent role of IGF-I in CNS axon growth and maturation and in oligodendrocyte function. In addition, normal formation of hippocampal granule cells and striatal parvalbumin-containing cells requires the presence of IGF-I. Inactivation of the *Igf1* gene did not affect the general anatomical organization of all CNS areas examined. Our findings can be interpreted as consequences of selective susceptibility of distinct cell types to IGF-I.

Experimental Procedures

Generation of *Igf1*$^{-/-}$ Mice

Production and general appearance of the *Igf1*$^{-/-}$, C57BL/6J-based mouse line used in this study has been described elsewhere (Powell-Braxton et al., 1993). Homozygous *Igf1*$^{-/-}$ mice were sacrificed at 2 months of age and compared with age-matched wild-type mice of identical strain and sex.

Histological Methods

Mice were sacrificed by CO_2 asphyxia; the brains were removed and immersion fixed for 2 days in 4% paraformaldehyde in 0.1 M phosphate buffer at 4°C and then cryoprotected in 30% sucrose. Serial coronal floating sections (40 μm) were cut on a sliding microtome and collected in 0.1 M phosphate buffer, 0.02% NaN_3 (pH 7.4) at 4°C for a maximum of 3 days before further processing.

For histological staining of myelin, sections were mounted on slides, stained with an aqueous solution of 0.2% eriochrome cyanine R and 0.4% $FeCl_3$ in 0.5% H_2SO_4, and differentiated in 1% aqueous NH_4OH (Clark, 1981). Measurements of the transection area of the anterior commissure and thickness of corpus callosum were done with an image analysis system (MCID, Imaging Research).

For electron microscope analysis of axon densities in white matter, deeply anesthetized mice were transcardially perfused with 2% paraformaldehyde/2.5% glutaraldehyde in 100 mM sodium phosphate buffer (pH 7.4). The brains were removed and postfixed in the same fixative for 3 days. Tissue blocks (approximately 1 mm^3) containing the anterior commissure or the medial part of corpus callosum were dissected, treated with 1% osmium tetroxide, dehydrated in ethanol, cleared in propylene oxide, and embedded in Eponate-12. Sections (60 nm) were cut using a diamond knife; these sections were mounted on a 300 mesh grid, stained with uranyl acetate and lead citrate, and studied in a Philips CM 12 electron microscope. From each section, 10 micrographs (10,000× magnification) were taken by systematically sampling the entire white matter area within the respective section. Axon density was calculated by counting myelinated and unmyelinated axons in each micrograph within a standard counting frame corresponding to 100 μm^2. Axons intersecting the borders of the frame were included in the count.

For immunohistochemistry, sections were incubated in 3% hydrogen peroxidein PBS for 30 min, then blocked/permeabilzed for 1 hr

in PBS containing either 0.1% Triton X-100, 10% normal horse serum, and 0.02% NaN_3 (solution A) or 1% Triton X-100, 2% bovine serum albumin, and 0.02% NaN_3 (solution B), followed by incubation with primary antibodies diluted in the respective blocking solution overnight at 4°C. The following antibodies were used: monoclonal antibodies against parvalbumin and calbindin D-28k (Swant, Bellinzona, Switzerland), both 1:9000 in solution A, against oligodendrocyte membranes (Chemicon, Temecula, CA), 1:500 in solution A, rabbit polyclonal antibodies against calretinin (Swant, Bellinzona, Switzerland), 1:9000 in solution A, against GFAP and TH (Chemicon, Temecula, CA), both 1:500 in solution B, against carbonic anhydrase II (a gift from Drs. Robert Skoff and Said Ghandour) at 1:250 in solution B, and goat polyclonal antibodies against ChAT (Chemicon, Temecula, CA), 1:500 in solution B. The ABC peroxidase method (Vector, Burlingame, CA) was used to detect bound antibodies, with 0.005% hydrogen peroxide and 0.05% diaminobenzidine as a substrate. Immunohistochemistry with these antibodies was done on every sixth serial section covering the entire extent of the respective region of interest. The total number of immunopositive neurons was estimated by multiplying the sum of the numbers of stained neurons on both sides with the correction factor six.

Every sixth serial coronal section through the hippocampus was stained with 0.1% cresyl violet and used to estimate the volumes of cell body layers of the dentate gyrus and CA1–4. Areas occupied by neuronal cell bodies in the two regions were measured with an image analysis system (MCID, Imaging Research). The volume was estimated by multiplying the total measured area of all analyzed sections by 40 μm (section thickness) and by the correction factor six. For estimates of the total striatal volume, the striatal area was measured in cresyl violet–stained serial sections.

Spinal cords were removed from bodies after immersion–fixation for 2 days, cryoprotected in sucrose, and then embedded in Tissue-Tek. Serial sections were cut at 18 μm thickness and stained with 0.1% cresyl violet and eriochrome cyanine R. The number of ventral horn motoneurons was estimated by counting clearly visible nucleoli in large cells with big nuclei and darkly stained cytoplasm in every fifth section from the fourth to the sixth cervical segment and multiplying the result by five. No correction was made for split nucleoli. Counts were performed in the fourth and fifth lumbar segment.

Acknowledgments

We thank Dr. Gilbert Keller, Linda Rangell, and Cara Warburton (all at Genentech, Incorporated) for technical assistance and Drs. Said Ghandour and Robert Skoff for the gift of the CA II antiserum. The studies at University of Southern California were supported by National Institutes of Health grants NS22933, AG10480, and AG09793, National Science Foundation grant BNS 9021255, and grants from the National Parkinson Foundation.

The costs of publication of this article were defrayed in part by the payment of page charges. This article must therefore be hereby marked *"advertisement"* in accordance with 18 USC Section 1734 solely to indicate this fact.

Received June 13, 1994; revised December 20, 1994.

References

Aizenman, Y., and De Vellis, J. (1987). Brain neurons develop in a serum and glial free environment: effects of insulin, insulin-like growth factor-I and thyroid hormone on neuronal survival, growth and differentiation. Brain Res. *406*, 32–42.

Aizenman, Y., Weischsel, M. E., Jr., and De Vellis, J. (1986). Changes in insulin and transferrin requirements of pure brain neuronal cultures during embryonic development. Proc. Natl. Acad. Sci. USA *83*, 2263–2266.

Altman, J., and Bayer, S. A. (1990a). Migration and distribution of two populations of hippocampal granule cell precursors during the perinatal and postanatal periods. J. Comp. Neurol. *301*, 365–381.

Altman, J., and Bayer, S. A. (1990b). Mosaic organization of the hippocampal neuroepithelium and the multiple germinal sources of dentate granule cells. J. Comp. Neurol. *301*, 325–341.

Ang, L. C., Bhaumick, B., Munoz, D. G., Sass, J., and Jurlink, B. H. (1992). Effects of astrocytes, insulin and insulin-like growth factor I on the survival of motoneurons in vitro. J. Neurol. Sci. *109*, 168–172.

Baimbridge, K. G., Celio, M. R., and Rogers, J. H. (1992). Calcium-binding proteins in the nervous system. Trends Neurosci. *15*, 303–308.

Baker, J., Liu, J.-P., Robertson, E. J., and Efstratiadis, A. (1993). Role of insulin-like growth factors in embryonic and postnatal growth. Cell *75*, 73–82.

Barres, B. A., and Raff, M. C. (1993). Proliferation of oligodendrocyte precursor cells depends on electrical activity in axons. Nature *361*, 258–260.

Barres, B. A., and Raff, M. C. (1994). Control of oligodendrocyte number in the developing rat optic nerve. Neuron *12*, 935–942.

Barres, B. A., Hart, I. K., Coles, H. S., Burne, J. F., Voyvodic, J. T., Richardson, W. D., and Raff, M. C. (1992). Cell death in the oligodendrocyte lineage. J. Neurobiol. *23*, 1221–1230.

Barres, B. A., Jacobson, M. D., Schmid, R., Sendtner, M., and Raff, M. C. (1993). Does oligodendrocyte survival depend on axons? Curr. Biol. *3*, 489–497.

Beck, K. D., Knusel, B., and Hefti, F. (1993). The nature of the trophic action of BDNF, des(1–3)IGF-1, and bFGF on mesencephalic dopaminergic neurons developing in culture. Neuroscience *52*, 855–866.

Bergmann, I., Nitsch, R., and Frotscher, M. (1991). Area-specific morphological and neurochemical maturation of non-pyramidal neurons in the rat hippocampus as revealed by parvalbumin immunocytochemistry. Anat. Embryol. *184*, 403–409.

Bondy, C. A. (1991). Transient IGF-I gene expression during the maturation of functionally related central projection neurons. J. Neurosci. *11*, 3442–3455.

Bondy, C., and Lee, W.-H. (1993). Correlation between insulin-like growth factor (IGF)-binding protein 5 and IGF-I gene expression during brain development. J. Neurosci. *13*, 5092–5104.

Bondy, C., Werner, H., Roberts, C. T., Jr., and LeRoith, D. (1992). Cellular pattern of type I insulin-like growth factor receptor gene expression during maturation of the rat brain: comparison with insulin-like growth factors I and II. Neuroscience *46*, 909–923.

Bothwell, M. (1982). Insulin and somatomedin MSA promote nerve growth factor-independent neurite formation by cultured chick dorsal root ganglionic sensory neurons. J. Neurosci. Res. *8*, 225–231.

Caroni, P., and Grandes, P. (1990). Nerve sprouting in innervated adult skeletal muscle induced by exposure to elevated levels of insulin-like growth factors. J. Cell Biol. *110*, 1307–1317.

Carson, M. J., Behringer, R. R., Brinster, R. L., and McMorris, F. A. (1993). Insulin-like growth factor increases brain growth and central nervous system myelination in transgenic mice. Neuron *10*, 729–740.

Celio, M. R. (1984). Parvalbumin as a marker for fast firing neurons. Neurosci. Lett. (Suppl.) *18*, 332.

Celio, M. R. (1990). Calbindin D-28k and parvalbumin in the rat nervous system. Neuroscience *35*, 375–475.

Clark, G. (1981). Staining Procedures. (Baltimore: Williams and Wilkins).

Clemmons, D. R., Jones, J. J., Busby, W. H., and Wright, G. (1993). Role of insulin-like growth factor binding proteins in modifying IGF actions. Ann. NY Acad. Sci. *692*, 10–21.

Collarini, E. J., Pringle, N., Mudhar, H., Stevens, G., Kuhn, R., Monuki, E. S., Lemke, G., and Richardson, W. D. (1991). Growth factors and transcription factors in oligodendrocyte development. J. Cell. Sci. (Suppl.) *15*, 117–123.

Czech, M. P. (1989). Signal transmission by insulin-like growth factors. Cell *59*, 235–238.

Daughaday, W. H. (1989). A personal history of the origin of the somatomedin hypothesis and recent challenges to its validity. Perspect. Biol. Med. *32*, 194–211.

Daughaday, W. H., and Rotwein, P. (1989). Insulin-like growth factors I and II: peptide, mRNA and gene structures, serum and tissue concentrations. Endocr. Rev. *10*, 68–91.

D'Ercole, A. J., Dai, Z., Xing, Y., Boney, C., Wilkie, M. B., Lauder,

J. M., Han, V. K. M., and Clemmons, D. R. (1994). Brain growth retardation due to the expression of human insulin-like growth factor binding protein-1 in transgenic mice: an in vivo model for the analysis of IGF function in the brain. Dev. Brain Res. *82*, 213–222.

DiCicco, E., and Black, I. B. (1988). Insulin growth factors regulate the mitotic cycle in cultured rat sympathetic neuroblasts. Proc. Natl. Acad. Sci. USA *85*, 4066–4070.

Eagleson, K. L., and Bennett, M. R. (1986). Motoneuron survival factor requirements during development : the change from immature astrocyte dependence to myotube dependence. Dev. Brain Res. *29*, 161–172.

Eagleson, K. L., Raju, T. R., and Bennett, M. R. (1985). Motoneuron survival is induced by immature astrocytes from developing avian spinal cord. Dev. Brain Res. *17*, 95–104.

Fagin, J. A., Fernandez-Mejia, C., and Melmed, S. (1989). Pituitary insulin-like growth factor-I gene expression: regulation by triiodothyronine and growth hormone. Endocrinology *125*, 2385–2391.

Froesch, E. R., Schmid, C., Schwander, J., and Zapf, J. (1985). Actions of insulin-like growth factors. Annu. Rev. Physiol. *47*, 443–467.

Gao, W.-Q., Heintz, N., and Hatten, M. E. (1991). Cerebellar granule cell neurogenesis is regulated by cell–cell interactions in vitro. Neuron *6*, 705–715.

Garcia-Segura, L. M., Perez, J., Pons, S., Rejas, M. T., and Torres-Aleman, I. (1991). Localization of insulin-like growth factor I (IGF-I)-like immunoreactivity in the developing and adult rat brain. Brain Res. *560*, 167–174.

Ghandour, M. S., Langley, O. K., Vincendon, G., Gombos, G., Filippi, D., Limozin, N., Dalmasso, D., and Laurent, G. (1980). Immunochemical and immunohistochemical study of carbonic anhydrase II in adult cerebellum: a marker for oligodendrocytes. Neuroscience *5*, 559–571.

Gyllensten, L., and Malmfors, T. (1963). Myelinization of the optic nerve and its dependence on visual function: a quantitative investigation in mice. J. Embryol. Exp. Morphol. *11*, 255–266.

Henderson, C. E., Camu, W., Mettling, C., Gouin, A., Poulsen, K., Karihaloo, M., Rullamas, J., Evans, T., McMahon, S. B., Armanini, M., Berkemeier, L., Philips, H. S., and Rosenthal, A. (1993). Neurotrophins promote motor neuron survival and are present in embryonic limb bud. Nature *363*, 266–270.

Hodgkinson, S. C., Spencer, G. S. G., Bass, J. J., Davis, S. R., and Gluckman, P. D. (1991). Distribution of circulating insulin-like growth factor-I (IGF-I) into tissues. Endocrinology *129*, 2085–2093.

Hughes, R. A., Sendtner, M., and Thoenen, H. (1993). Members of several gene families influence survival of rat motoneurons in vitro and in vivo. J. Neurosci. Res. *36*, 663–671.

Hughes, S. M., Lillien, L. E., Raff, M. C., Rohrer, H., and Sendtner, M. (1988). Ciliary neurotrophic factor induces type-2 astrocyte differentiation in culture. Nature *335*, 70–73.

Hynes, M. A., Brooks, P. J., Van Wyk, J. J., and Lund, P. K. (1988). Insulin-like growth factor II messenger RNAs are synthesized in the choroid plexus of the rat brain. Mol. Endocrinol. *2*, 47–54.

King, R. A., Smith, R. M., Meller, D. J., Dahlenburg, G. W., and Lineham, J. D. (1988). Effect of growth hormone on growth and myelination in the neonatal hypothyroid rat. J. Endocrinol. *119*, 117–125.

Knüsel, B., Michel, P. P., Schwaber, J., and F. Hefti (1990). Selective and nonselective stimulation of central cholinergic and dopaminergic development in vitro by nerve growth factor, basic fibroblast growth factor, epidermal growth factor, and the insulin-like growth factors. J. Neurosci. *10*, 558–570.

Lee, W.-H., Javedan, S., and Bondy, C. A. (1992). Coordinate expression of insulin-like growth factor system components by neurons and neuroglia during retinal and cerebellar development. J. Neurosci. *12*, 4737–4744.

Lee, W.-H., Michels, K. M., and Bondy, C. A. (1993). Localization of insulin-like growth factor binding protein-2 messenger RNA during postnatal brain development: correlation with insulin-like growth factors I and II. Neuroscience *53*, 251–265.

LeVine, S. M., and Goldman, J. E. (1988). Embryonic divergence of oligodendrocyte and astrocyte lineages in developing rat cerebrum. J. Neurosci. *8*, 3992–4006.

Liu, J.-P., Baker, J., Perkins, A. S., Robertson, E. J., and Efstratiadis, A. (1993). Mice carring null mutations of the genes encoding insulin-like growth factor I (*Igf-1*) and type I IGF receptor (*Igf1r*). Cell *75*, 59–72.

Mathews, L. S., Norstedt, G., and Palmiter, R. D. (1986). Regulation of insulin-like growth factor gene expression by growth hormone. Proc. Natl. Acad. Sci. USA *83*, 9343–9347.

Matthieu, J. M., Widmer, S., and Hershkowitz, N. (1973). Biochemical changes in mouse brain composition during myelination. Brain Res. *55*, 391–402.

Mattson, M. P., Rychlik, B., Chu, C., and Christakos, S. (1991). Evidence for calcium-reducing and excito-protective roles for the calcium-binding protein calbindin-D28k in cultured hippocampal neurons. Neuron *6*, 41–51.

McMorris, F. A., and Dubois-Dalcq, M. (1988). Insulin-like growth factor I promotes cell proliferation and oligodendroglial commitment in rat glial progenitor cells dveloping in vitro. J. Neurosci. Res. *21*, 199–209.

McMorris, F. A., Furlanetto, R. W., Mozell, R. L., Carson, M. J., and Raible, D. W. (1990). Regulation of oligodendrocyte development by insulin-like growth factors and cyclic nucleotides. Ann. NY Acad. Sci. *605*, 101–109.

McMorris, F. A., Smith, T. M., DeSalvo, S., and Furlanetto, R. W. (1986). IGF-I/somatomedin-C: a potent inducer of oligodendrocyte development. Proc. Natl. Acad. Sci. USA *83*, 822–826.

Morell, P., Greenfield, S., Constantino-Ceccarini, E., and Wisniewski, H. (1972). Changes in protein composition of mouse brain myelin during development. J. Neurochem. *19*, 2545–2554.

Mozell, R. L., and McMorris, F. A. (1991). Insulin-like growth factro I stimulates oligodendrocyte development and myelination in rat brain aggregate cultures. J. Neurosci. Res. *30*, 382–390.

Neff, N. T., Prevette, D., Houenou, J. L., Lewis, M. E., Glicksman, M. A., Yin, Q.-W., and Oppenheim, R. W. (1993). Insulin-like growth factors: putative muscle-derived trophic agents that promote motoneuron survival. J. Neurobiol. *24*, 1578–1588.

Noble, M., and Wolswijk, G. (1992). Development and regeneration in the O-2A lineage: studies in vitro and in vivo. J. Neuroimmunol. *40*, 287–93.

Noble, M., Ataliotis, P., Barnett, S. C., Bevan, K., Bogler, O., Groves, A., Jat, P., Wolswijk, G., and Wren D. (1991). Development, regeneration, and neoplasia of glial cells in the central nervous system. Ann. NY Acad. Sci. *633*, 35–47.

Noguchi, T. (1991). Retarded cerebral growth of hormone-deficient mice. Comp. Biochem. Physiol. *98*, 239–248.

Noguchi, T., Sugisaki, T., Takamatsu, K., and Tsukada, Y. (1982a). Factors contributing to the poor myelination in the brain of the Snell dwarf mouse. J. Neurochem. *39*, 1693–1699.

Noguchi, T., Sugisaki, T., and Tsukada, Y. (1982b). Postanatal action of growth and thyroid hormones on the retarded cerebral myelinogenesis of Snell dwarf mice (dw). J. Neurochem. *38*, 257–263.

Noguchi, T., Sugisaki, T., and Tsukada, Y. (1985). Microcephalic cerebrum with hypomyelination in the growth hormone-deficient mouse (lit). Neurochem. Res. *10*, 1097–1106.

Ocrant, I., Fay, C. T., and Parmelee, J. T. (1990). Characterization of insulin-like growth factor binding proteins produced in the rat central nervous system. Endocrinology *127*, 1260–1267.

Ooi, G. (1990). Insulin-like growth factor binding proteins (IGFBPs): more than just 1, 2, 3. Mol. Cell. Endocrinol. *71*, 39–43.

Powell-Braxton, L., Hollinghead, P., Warburton, C., Dowd, M., Pitts-Meek, S., Dalton, D., Gillett, N., and Stewart, T. A. (1993). IGF-I is required for normal embryonic growth in mice. Genes Dev. *7*, 2609–2617.

Raff, M. C. (1992). Social controls on cell survival and cell death. Nature *356*, 397–400.

Ralphs, J. R., Wylie, L., and Hill, D. J. (1990). Distribution of insulin-like growth factor peptides in the developing chick embryo. Development *109*, 51–58.

Rechler, M. M., and Nissley, S. P. (1990). Insulin-like growth factors. Handbook Exp. Pharmacol. *95*, 263–367.

Rechler, M. M., and Brown, A. L. (1992). Insulin-like growth factor binding proteins: gene structure and expression. Growth Regul. *2*, 55–68.

Résibois, A., and Rogers, J. H. (1992). Calretinin in rat brain: an immunohistochemical study. Neuroscience *46*, 101–134.

Rotwein, P., Burgess, S. K., Milbrandt, J. D., and Krause, J. E. (1988). Differential expression of insulin-like growth factor genes in rat central nervous system. Proc. Natl. Acad. Sci. USA *85*, 265–269.

Sara, V. R., and Hall, C. (1990). Insulin-like growth factors and their binding proteins. Physiol. Rev. *70*, 591–614.

Siddle, K. (1992). The insulin receptor and type I IGF receptor: comparison of structure and function. Prog. Growth Factor Res. *4*, 301–320.

Solbach, S., and Celio, M. R. (1991). Ontogeny of the calcium binding protein parvalbumin in the rat nervous system. Anat. Embryol. *184*, 103–124.

Stylianopoulou, F., Herbert, J., Soares, M. B., and Efstratiadis, A. (1988). Expression of the insulin-like growth factor II gene in the choroid plexus and the leptomeninges of the adult rat central nervous system. Proc. Natl. Acad. Sci. USA *85*, 141–145.

Sugisaki, T., Noguchi, T., and Tsukada, Y. (1985). Cerebral myelinogenesis in the Snell dwarf mouse: stimulatory effects of GH and T4 restricted to the first 20 days of postnatal life. Neurochem. Res. *10*, 767–778.

Tauber, H., Waehneldt, T. V., and Neuhoff, V. (1980). Myelination in rabbit optic nerves is accelerated by artificial eye opening. Neurosci. Lett. *16*, 235–238.